KINETICS STUDY OF DROPLET SWELLING IN BOF STEELMAKING

Elaine Chen & Kenneth Coley
McMaster University, Canada

ABSTRACT

Previous work in the authors' laboratory, described elsewhere in this conference, has shown that an understanding of droplet swelling is essential in predicting droplet residence times in BOF steelmaking. Several workers have observed swelling of high carbon droplets when exposed to oxidizing slags. In the present work the authors present data on swelling rates measured by x-ray fluoroscopy and compare this with the total volume of gas evolved during the reaction. It is shown that only a small percentage of the gas generated is retained in the droplet to contribute to swelling.

The gas generation rate is shown to be controlled by the rate of nucleation of CO bubbles inside the droplet. The critical supersaturation pressure for nucleation is found to be two orders of magnitude less than predicted from theory, which is in keeping with many other studies on nucleation of gasses in liquids. However the effect of surface tension, temperature and saturation pressure show quantitative agreement with theory.

The influences of various experimental parameters on gas nucleation will be discussed.

INTRODUCTION

Considerable attention [see ref. 1 to 23] has been paid to the reaction between molten iron oxide containing slag and iron droplets or solid carbon due to the critical roles it plays in various metallurgical processes, like basic oxygen furnace (BOF) steelmaking, bath smelting reduction processes, as well as electric arc furnace (EAF) steelmaking. During the last two decades, numerous studies have been carried out on droplets, for which the size remains constant. Under this circumstance, a gas halo was formed around the droplet. The proposed possible rate determining steps could be in sequence: mass transfer of Fe^{2+} and O^{2-} in the liquid slag phase, chemical reaction at slag gas interface ($CO + FeO = Fe + CO_2$) gas phase transport in gas halo, chemical reaction at carbon gas interface ($CO_2 + \underline{C} = 2CO$). Empirical equations and mathematical models have been established for each of these individual steps, which are well understood. However, another important phenomenon, that the droplet will swell when it reacts with iron oxide containing slag has not been paid the same attention. Knowledge of the extent of droplet swelling is essential in predicting residence times in BOF steelmaking [24]. To date, very few studies [12, 13] have been done on the measurement of swelling rate of the droplets in the slag, and there is insufficient data available to predict swelling rates.

A similar phenomenon, called *boiling* is observed when droplets pass through oxidizing gases (such as mixtures of CO and CO_2, or O_2) [see ref. 1 to 23]. Baker *et al.* first [25, 26, 27] observed iron droplet's swelling when passing through a gas mixture of oxygen and helium. The droplets were observed to explode due to CO nucleation inside the metal. A supersaturation of 5×104 atm [28, 30] was calculated for CO nucleation, which is two orders higher than the experimental measurements. The high supersaturation pressure makes homogeneous nucleation of CO bubbles inside metal impossible. Various explanations have been proposed. Early work by Levine [38, 39, 40] investigated the effect of the surface active element, oxygen, which will decrease the surface tension and the work needed for the formation of an embryo inside the melt. However, even if oxygen decreases the surface tension from 1.6 N/m to 1 N/m, the calculated supersaturation pressure is still extremely high (25000 atm) [41]. Gare *et al.* [5] proposed that the nucleation was heterogeneous due to entrainment of gas in the molten droplet when it fell through furnace at the start of the experiment. The entrained gas acted as a gas nucleus for heterogeneous nucleation. Robertson and Jenkins [29] proposed that the nucleation is neither homogeneous nor heterogeneous, and invoked vortex nucleation. They also mentioned that oxygen has a large effect on interfacial turbulence thus benefiting CO nucleation.

Although there are some explanations for the nucleation of CO bubbles inside the droplets, the rate still could not be predicted. In this work we will re-examine the classical nucleation equation in light of our experimental results in an attempt to render nucleation rate predictable.

EXPERIMENTAL DETAILS

The experimental arrangement is shown schematically in Figure 1. A vertical resistance heated tube furnace, with an 80 mm diameter alumina working tube was used for all the experiments. The tube ends are sealed with O-rings and water cooled stainless steel caps. Two rectangular holes were cut on the stainless shell of the furnace in order to allow the minimum absorption of X-rays. Slag samples were prepared by mixing of reagent grade MgO, CaO, SiO_2 and FeO powders. 60 g of sample was loaded into a 45 mm diameter magnesium oxide crucible. An alumina dispensing tube was placed inside the working tube, 25 mm above the crucible. The hole at the base of dispensing tube ensures that the iron pellet melts before entering the slag. A thermocouple (type B: Pt-6 pct Rh/Pt-30 pct Rh) was inserted to the bottom of the crucible to measure the temperature. Temperature was controlled automatically by a programmable EUROTHERM controller.

During heating de-oxidized oxygen flowed continuously through the furnace. Once the desired temperature was reached, the furnace was sealed. An approximately one gram iron pellet held by a Nd magnet at the top of the alumina injection tube was released, after about 40 s, the droplet melted and fell through the 5 mm hole at the bottom of the dispensing tube. The reaction started immediately, photos were taken by X-ray Fluoroscopy (GE OEC Medical Systems, Inc.), and gas evolution measured by the pressure transducer and recorded on a PC. A maximum measurable range of 2 psi of differential pressure transducer was used to measure the pressure change caused by the gas evolution during the reaction.

RESULTS

Droplet Swelling Rate

The reaction behavior was observed for a droplet containing C=3.71%, S=0.0063%. On entering the slag, due to the fast external decarburization rate, the droplet floated on the surface of the slag rather than falling to the bottom of the crucible. A gas halo was formed around the droplet once it contacted the slag. Meanwhile slag foam was also observed. The diameter of droplets increased to 1.5 times the original. The fast decarburization reaction on slag surface lasted for 4s, then droplets fell back into the slag, after which the reactive drop still gave off gas so that a maximum 50 mm of foam was observed, which lasted for 15s before it collapsed.

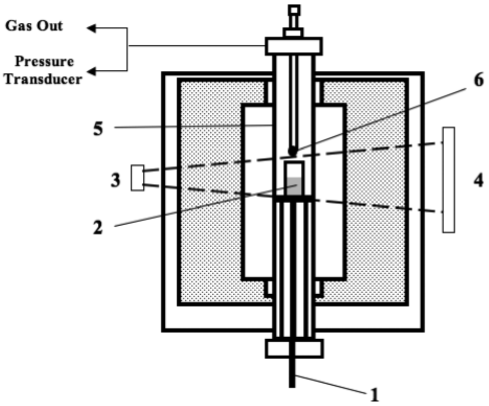

Figure 1: Schematic diagram of the experimental setup- 1. Thermocouple 2.Slag 3.X-ray Generator 4. Image Intensifier 5.Working Tube 6. Iron Pellet

Faster swelling of droplets in the slag was observed by dropping 1g or 2 g of metal with C=2.64%, S=0.022%. After an incubation time of about 2s, the diameter became 4 times bigger than the original size for 2 g of metal, and 3 times for 1g of metal, then shrunk to 1.5 times the original size, and continued to react with the slag for 2 s before falling down to the bottom of the crucible. The swelling rate with time for 1g and 2 g droplet is shown in Figure 2.

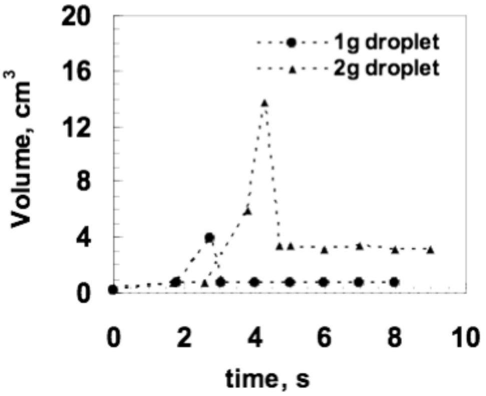

Figure 2: Swelling rate for 1 g and 2 g size of pig iron at T=1773 K

CO Evolution Rate

The Effect of Iron Droplet Size

At fixed metal droplet compositions (C=2.64%, S=0.022%) and slag (CaO/SiO_2=1.2, MgO=12%, FeO=20%) chemistry, a series of experiments were designed to study the dependence of CO evolution rate on droplet size. In each experiment, the CO evolution rate was measured at T=1773 K. Figure 3 shows the dependence of CO evolution rate on the size of iron pellet, it increases linearly with droplet mass. Comparing Figure 2 and 3, for a 1 g droplet, 10% of the generated CO causes the droplet to swell to maximum size of 3.88 cm^3, 33% for a 2 g metal droplet.

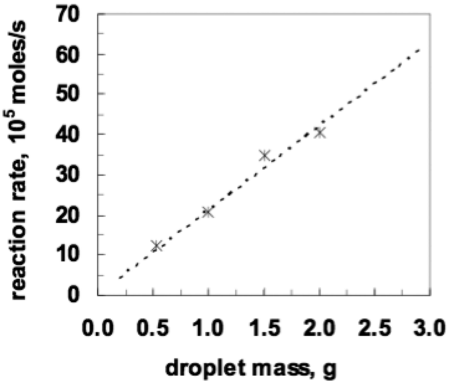

Figure 3: Dependence of CO evolution on pig iron size at T=1773 K

The Effect of Temperature

The temperature dependence of CO evolution was investigated at C=2.91%, S=0.013%. The slag compositions are CaO/SiO_2=1.2, MgO=12%, FeO=3, 10, 20%. The results are depicted in Figure 4.

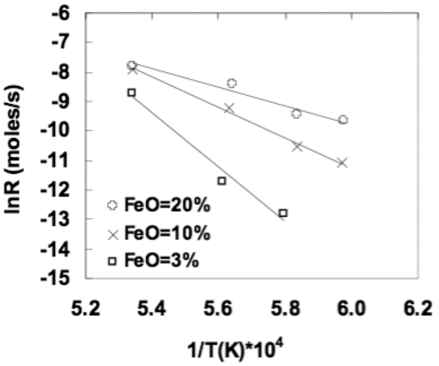

Figure 4: Dependence of CO evolution rate on temperature

The Effect of FeO Content

CO evolution rate was studied for slags with 3 to 30 wt pct FeO at different temperatures. Figure 5 shows the dependence of CO evolution rate on the iron oxide content.

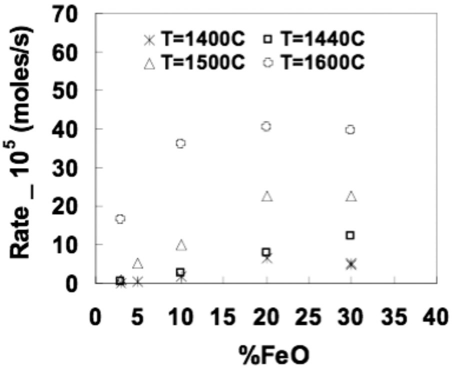

Figure 5: Dependence of CO evolution rate on FeO content

The Effect of Sulphur Content

At fixed oxygen potential, CO evolution rate was studied at the range of S content from 0 wt pct to 0.194 wt pct. The rate goes through a maximum with respect to sulphur content in the metal.

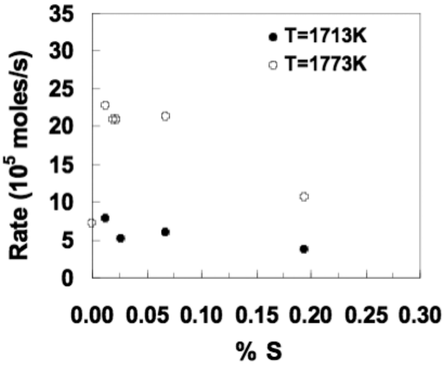

Figure 6: Dependence of CO evolution rate on S content

DISCUSSION

CO Nucleation inside the Metal

There are two mechanisms for the carbon oxygen reaction when iron droplets react with iron oxide containing slag. One is the surface reaction where carbon is removed at the surface of the droplet. Under this circumstance, a gas halo is formed around the droplets and the size of droplet does not change. Another involves the nucleation of CO bubbles inside the metal, in which case the droplet will swell. Whether or not CO bubbles will nucleate inside the metal depends on the balance between the diffusion rate of oxygen transfer from the slag into the bulk of the metal and the rate of the mass transfer of carbon from the bulk to the surface. If the oxygen supply rate is higher than carbon diffusion rate, there is a possibility for CO nucleation inside the metal which causes droplet swelling. The carbon and oxygen reaction inside the metal is expressed by:

$$\underline{C} + \underline{O} = CO_{(g)} \tag{1}$$

Nucleation of CO bubbles involves the clustering process: carbon and oxygen firstly form a metastable CO cluster by reaction 2,

$$\left.\begin{array}{l}\underline{C} \rightarrow C^* \\ \underline{O} \rightarrow O^*\end{array}\right\} \rightarrow (CO)^* \tag{2}$$

As the clustering process proceeds, the liquid metal becomes supersaturated with CO embryos, local fluctuation sets CO embryos growing into bubbles. This process is quite similar to liquid vapor phase change phenomena [42, 43] and the nucleation rate is given by:

$$J_s = N_0 \exp[\frac{-\Delta H}{kT}][\frac{3\sigma}{\pi m}]^{\frac{1}{2}} \exp[\frac{-16\pi\sigma^3}{3kT[P_{ve} - P_L]^2}] \tag{3}$$

Where: N_0: is the number concentration of CO embryos in the liquid; σ is surface tension at liquid gas interface; ΔH is heat of formation of one CO molecule; m is the mass of one molecule; T is temperature, in Kelvin, k is Boltzman constant; P_{ve} is the pressure in the vapor bubble at equilibrium; P_L is liquid pressure.

The number concentration of CO embryos depends on the smaller of the concentration of oxygen or carbon, in the case of a high carbon activity in the metal, it depends on oxygen concentration reached during the incubation time. The X-ray observations showed that for each size of iron droplet, it requires time, τ, to establish the steady stage nucleation conditions. In this study it took about 1.8 s for a 1 g droplet rise out of the liquid slag, during this period, oxygen diffused into metal droplet. Taking the oxygen mass transfer co-efficient as $3.8*10^{-3}$ moles/cm^{2}s as proposed by Molloseau and Fruehan [12, 13], the calculated activities of carbon and oxygen as 6.525 and 0.062, respectively, and the CO pressure at equilibrium as 163 atm, the calculated nucleation rate is:

$$J_s = 2.04*1038 \exp\left[-\frac{217}{10^{-6}}\right] \approx 0 \qquad (4)$$

The classical nucleation rate equation predicts no bubble formation, as has also been found by several other workers [28, 29, 30]. Heterogeneous nucleation on inclusions is unlikely because the metal is very clean. From the calculation in Equation 5, it can be seen that the nucleation rate goes to zero because the energy term inside the exponential is too large. This observation led most previous workers to conclude that an extremely high supersaturation pressure (two orders higher than experimental measurements) is needed for the formation of CO bubbles, which is in keeping with many other studies on nucleation of gasses in liquids [44, 45].

Assuming a value for σ of 0.9 N/m [46, 47], the minimum radius of stable bubble nucleus is $r=1.97*10^{-7}$ m, which contains about $2.2*10^7$ molecules, now we can see where the problem is. The large number of molecules makes formation of such nucleus impossible. Levine [38, 39, 40] proposed that doubly charged chemisorbed oxygen ions in the surface layer of spherical CO embryos decreased the surface tension and thus decreased the energy barrier for nucleation. The reduction magnitude of surface tension is not known, but it is reasonable to set $\sigma = \psi\sigma 0$. $\psi=0.023$ was obtained based on one of the measured CO evolution rate, ψ value between 0 and 1 has been shown to be reasonable in several systems [39, 44, 45]. Re-calculating the bubble radius, $r=2.64*10^{-9}$ m, this bubble would contain 54 molecules. This is consistent with studies of dissolved gas in water where there are typically a few hundred molecules in the critical nucleus [44]. The modified nucleation rate Equation is expressed by:

$$J_s = N_0 \exp\left(\frac{-\Delta H}{kT}\right)\left[\frac{3(\psi\sigma_0)}{\pi m}\right]^{\frac{1}{2}} \exp\left[\frac{-16\pi(\psi\sigma_0)^3}{3kT[P_{ve} - P_L]^2}\right] \qquad (5)$$

The CO generation rate can be calculated now:

$$R_G = J_s \cdot \left(\frac{n_e}{N_A}\right) \cdot V_0 \qquad (6)$$

where: R_G is CO generation rate, moles/s; J_s is CO nucleation rate, /cm^{3}s; V0 is the original droplet volume, cm^3; n_e is the number of molecules in an embryo; N_A is Avogadro number.

Figure 4 shows the effect of droplets mass on CO evolution rate. In Equation 6, the pre-exponential term has little effect on the nucleation rate, the terms inside the exponential, temperature, T, surface tension, σ and supersaturation pressure, ΔP change less than 1%, J may rise by many orders of magnitude. If T, σ an d ΔP were kept the same, CO evolution rate should increase linearly with droplet mass, this is in good agreement with our experimental results.

The effect of sulphur on CO evolution rate is quiet complicated. On the one hand, it decreases metal surface tension, and reduces the energy barrier for the nucleation, thereby accelerating the decarburization rate. On the other hand, sulfur segregates to the surface and leads to poisoning of the reaction sites. Due to the poisoning of the reaction sites, less oxygen would transfer into the metal droplets, causing a lower supersaturation pressure, which would decrease the CO nucleation rate. Due to two competing effects, a maximum value of CO evolution rate should be observed at specific sulphur content. In this study, at T=1773 K, the maximum rate was found at S=0.0126 wt pct.

Gas generation rate is controlled by the rate of nucleation of CO bubbles, for a given bulk compositions of slag, CO evolution rate increases exponentially with temperature according to Equation 5, this fits well with our results, see Figure 4. Figure 7 shows the comparison between experimental measurements and the calculated values from Equation 6, taking ψ=0.023, the agreement is excellent for T=1773 K and very reasonable for other temperatures, it is possible that a different value of ψ should be used for various temperatures.

CONCLUSIONS

- For iron-carbon droplets reacting with oxidizing slag, the dependency of CO evolution rate on original droplet size indicates that the rate determining step is the nucleation of CO bubbles.
- Classical nucleation theory shows excellent qualitative agreement with the observed gas generation rates. However, to obtain reasonable predictions of nucleation rates, the metal surface tension has to be decreased by a factor of about 40. This is consistent with observation of gas nucleation behavior in a number of different systems.

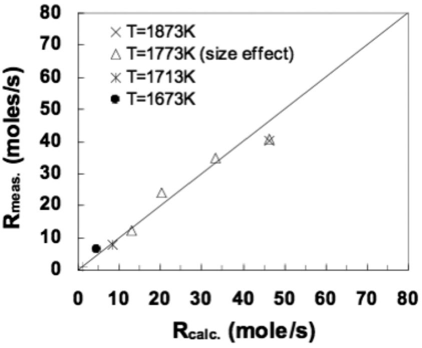

Figure 7: Comparison between theoretical predictions and experimental measurements

AKNOWLEDGEMENTS

The authors acknowledge the financial support of this work by NSERC and Steel Research Center of McMaster University. E. Chen wishes to thank Dr. F. Ji for his great help in the experimental setup.

REFERENCES

Meyer, H. W., Porter, W. F., Smith, G. C. & Szekely, J. (1968). Slag-Metal Emulsions and their Importance in BOF Steelmaking, *Journal of Metals*, July, pp. 35-42. [1]

Kozakevitch, P. (1969). Foams and Emulsions in Steelmaking, *Journal of Metals*, July, pp.57-68 [2]

Mulholland, E. W., Hazeldean, G. S. F. & Davies, M. W. (1973). Visualization of Slag Metal Reactions by X-ray Fluoroscopy: Decarburization in Basic Oxygen Steelmaking, *Journal of the Iron and Steel Institute*, September, pp. 632-639. [3]

Gaye, H. & Riboud, P. V. (1977). *Oxidation Kinetics of Iron Alloy Drops in Oxidizing Slags*. Metallurgical and Materials Transactions B: 8B, pp. 409-415. [4]

Gare, T. & Hazeldean, G. S. F. (1981). *Basic Oxygen Steelmaking: Decarburization of Binary Fe-C Droplets and Ternary Fe-C-X Droplets in Ferruginous Slags*. Ironmaking and Steelmaking, No. 4, pp. 169-181. [5]

Min, D. J, Han, J. W. & Chung, W. S. (1999). *Rate of Reduction of FeO in Slag by Fe-C Drops*. Metallurgical and Materials Transactions B: 30B, p. 215. [6]

Min, D. J. & Fruehan, R. J. (1992). *Rate of Reduction of FeO in Slag by Fe-C Drops*. Metallurgical and Materials Transactions B: 23B, pp. 29-37. [7]

Sarma, B., Cramb, A. W., & Fruehan, R. J. (1996). *Reduction of FeO in Smelting Slags by Solid Carbon: Experimental Results*. Metallurgical and Materials Transactions B, 27B, pp.717-730. [8]

Krishna Murthy, G. G., Sawada, Y. & Elliott, J. F. (1993). *Reduction of FeO Dissolved in CaO-SiO_2-Al_2O_3 Slags by Fe-C Droplets*. Ironmaking and Steelmaking, Vol. 20, No. 3, pp. 179-190. [9]

Krishna Murthy, G. G., Hasham, A. & Pal, U. B. (1993). *Reduction Rates of FeO Dissolved in CaO-SiO_2-Al_2O_3 Slags by Fe-C Droplets*. Ironmaking and Steelmaking, Vol. 20, No. 3, pp. 191-200. [10]

Krishna Murthy, G. G., Hasham, A. & Pal, U. B. (1994). *Removal of FeO during Foaming of CaO-SiO_2-Al_2O_3 Slags by Low Carbon Iron Melts*. ISIJ, pp. 408-413. [11]

Molloseau, C. L. (1999). *Waste Oxide Recycling during Oxygen Steelmaking*. PhD thesis, Carnegie-Mellon University, Pittsburgh, PA. [12]

Molloseau, C. L. & Fruehan, R. J. (2002). *The Reaction Behavior of Fe-C-S Droplets in CaO-SiO_2-MgO-FeO Slags*. Metallurgical and Materials Transactions B, Vol. 33B, June, pp. 335-344. [13]

Davies, M. W., Hazeldean, G. S. F. & Smith, P. N. (1973). *Kinetics of Reaction between Liquid Iron Oxide Slags and Carbon*. Physical chemistry of process metallurgy: the Richardson conference, papers presented at the July 1973 conference, pp. 95-107. [14]

Grezl, K. & Molloy, N. A. (1977). *Decarburization Reaction Model*. Second Australian Conference on Heat and Mass Transfer, pp. 461-468. [15]

Davies, M. W., Hazeldean, G. S. F. & Smith, P. N. (1974). *Kinetics of Reaction between Liquid Iron Oxide Slags and Carbon*. pp. 95-107. [16]

Acheson, R. & Hills, A. W. D. *Rate-Controlling Mechanisms in Basic Oxygen Steelmaking*. pp. 153-163. [17]

Paul, A., Deo, B. & Sathyamurthy, N. (1994). *Kinetics Model for Reduction of Iron Oxide in Molten Slags by Iron Carbon Melt*. Steel Research, No. 10, pp. 414-420. [18]

Smith, R. H. & Fruehan, R. J. (1999). *The Effect of Carbon Content on the Rate of Reduction of FeO in Slag Relevant to Iron Smelting*. Steel Research, No. 8+9, pp. 283-295. [19]

Upadhya, K., Sommerville, I. D. & Grieveson, P. (1980). *Kinetics of Reduction of Iron Oxide in Slag by Carbon in Iron: Part 2 Effect of Carbon Content of Iron and Silica Content of Slag*. Ironmaking and Steelmaking, No. 1, pp. 33-36. [20]

Sato, A., Aragane, G., Kamihira, K. & Yoshimatsu, S. (1987). *Reducing Rates of Molten Iron Oxide by Solid Carbon or Carbon in Molten Iron*. Transactions ISIJ, Vol. 27, pp. 789-796. [21]

Paramguru, R. K., Ray, H. S. & Basu, P. (1996). *Kinetics of Reduction of FeO in CaO-SiO_2-FeO Slags Part I: Reduction by Solute Carbon*. Vol. 23, No. 4, pp. 328-334. [22]

Seo, J-D. & Kim, S-H. (1998). *Reaction Mechanism of FeO Reduction by Solid and Dissolved Carbon*. Steel Research, Vol. 69, No. 8, pp. 307-311. [23]

Brooks, G., Pan, Y., Subagyo & Coley, K. (2005). *Modeling of Trajectory and Residence Time of Metal Droplets in Slag Metal Gas Emulsions in Oxygen Steelmaking*. Metallurgical and Materials Transactions B, 36B, pp. 525-535. [24]

Baker L. A. & Ward, R. G. (1967). Reaction of an Iron Carbon Droplet during Free Fall through Oxygen, *Journal of The Iron and Steel Institute*, July, pp. 714-717. [25]

Baker, L. A., Warner, N. A. & Jenkins, A. E. (1967). *Decarburization of a Levitated Iron Droplet in Oxygen*. Transactions of The Metallurgical Society of AIME, Vol. 239, pp. 857-864. [26]

Baker, L. A., Warner, N. A. & Jenkins, A. E. (1964). *Kinetics of Decarburization of Liquid Iron in an Oxidizing Atmosphere Using the Levitation Technique*. Trans. AIME, Vol. 230, pp. 1228-1235. [27]

Kaplan, R. S. & Philbrook, W.O. (1972). *The Rate of CO Bubble Nucleation at Oxide Metal Interfaces within Liquid Iron Alloys*. Metallurgical transactions, Vol. 3, pp. 483-487. [28]

Robertson, D. G. C. & Jenkins, A. E. (1970). *The Reaction of Liquid Iron and its alloys in Pure Oxygen*. Heterogeneous Kinetics at Elevated Temperatures, pp. 393-408. [29]

Kaddah, N. H. E. L. & Robertson, D. G. C. (1977). Homogeneous Nucleation of Carbon Monoxide Bubbles in Iron Drops, *Journal of Colloid and Interface Science*, pp. 349-360. [30]

Kaddah, N. H. E. L. & Robertson, D. G. C. (1977). *Equilibria in Reactions of CO and CO_2 with Dissolved Oxygen and Carbon in Liquid Iron*. Metallurgical and Materials Transactions B, pp. 569-579. [31]

Kaddah, N. H. E. L. & Robertson, D. G. C. (1988). *The Nucleation of CO Bubbles in Molten Iron Carbon Drops Reacting with Oxidizing Gases*. Metallurgical and Materials Transactions B: 19B, pp. 831-837. [32]

Panda, D. K. & Robertson, D. G. C. (1994). *Physical Modeling of Metal Drop Slag Reactions with Gas Evolution*. Steelmaking conference proceedings, 1994, pp. 443-456. [33]

Distin, P. A., Hallett, G. D. & Richardson, F. D. (1968). Some Reactions between Drops of Iron and Flowing Gases, *Journal of the Iron and Steel Institute*, August, pp. 821-833. [34]

Roddis, P. G. (1973). Mechanism of Decarburization of Iron Carbon Alloy Drops Falling through an Oxidizing Gas, *Journal of the Iron and Steel Institute*, January, pp. 53-58. [35]

Gao, K., Sahajwalla, V. & Dry, R. (1998). *Carbon Boiling Phenomenon and Oxygen Adsorption by Metal Drops in Direction Iron Smelting*. ICSTI/Ironmaking conf. proc., pp. 1489-1499. [36]

Richardson, F. D. (1974). *Physical Chemistry of Melts in Metallurgy*. Vol. 2, pp. 426-461. [37]

Levine, H. S. (1972). Formation of Vapor Nuclei in High Temperature Melts, *The Journal of Physical Chemistry*, Vol. 76, No. 18, pp. 2609-2614. [38]

Levine, H. S. (1973). *Homogeneous Nucleation of CO Bubbles in Fe-C-O Melts*. Metallurgical Transactions, Vol. 4, pp: 777-782. [39]

Levine, H. S. (1974). *Surface Structure Concepts in the Theory of Homogeneous Bubble Nucleation*. Metallurgical transactions B, Vol. 5, pp. 953-955. [40]

Kwak, Ho-Young & Oh, Si-Doek (1998). A Model of Homogeneous Bubble Nucleation of CO Bubbles in Fe-C-O Melts, *Journal of Colloid and Interface Science*, Vol. 198, pp. 113-118. [41]

Volmer, M. (1939). *Kinetics of Phase Formation*. ATI No.81935 (F-TS-7068-RE) Translated from Kinetic der Phasenbildung Verl-Steinkopff Dresden, pp. 149-154. [42]

Van. P. Carey (2008). *Liquid –Vapor Phase Change Phenomena*. second Edition. [43]

Bowers, P. G., Bar-Eli, K. & Noyes, R. M. (1996). Unstable Supersaturated Solutions of Gases and Nucleation Theory, *Journal of Chemical Society*, Faraday Transactions, 92(16), pp. 2843-2849. [44]

Lubetkin, S. D. (2003). *Why Is It Much Easier to Nucleate Gas Bubbles than Theory Predicts T?*. Langmuir, 19, pp. 2575-2587. [45]

Jimbo, U., Sharan, A. & Cramb, A. W. (1994). *The Surface and Interfacial Tensions of Steel Alloys Containing Nickel or Carbon and Sulphur*. Iron and Steelmaker, pp. 48-55. [46]

Cramb, Alan W. & Jimbo, U. (1989). *Calculation of the Interfacial Properties of Liquid Steel-Slag Systems*. Steel Research, 60, No. 3+4, pp. 157-165. [47]